NUMERICAL PREDICTION OF HEAT TRANSFER ON TRANSONIC TURBINE BLADES AT OFF DESIGN OPERATING CONDITIONS

Dorin STANCIU[1], Alexandru DOBROVICESCU[2]

Lucrarea analizează performanţele modelelor de turbulenţă v2-f (*Lien and Durbin, 1996*) *şi ζ-f* (*Hanjalic et al., 2004*) *în simularea numerică a transferului convectiv de căldură pentru curgerea turbulentă transonică printr-o reţea bidimensionala de palete de turbină. Fluxul turbulent de căldură a fost modelat considerând o valoare constantă a numărului Prandtl turbulent sau cu ajutorul relaţiei algebrice a difuzivităţii termice turbulente propusă de Rokni şi Sunden* (*2003*)*. Rezultatele numerice evidenţiază că în zonele de existenţă ale stratului limită turbulent, coeficientul de transfer convectiv de căldură este corect simulat de ambele modele de turbulenţă Cu toată utilizarea condiţiei de constrângere a lui Durbin, in punctul de stagnare fluxul de căldură este supraevaluat prin utilizarea ipotezei* Pr_t*=const., dar relaţia algebrică a lui Rokni şi Sunden corectează această problemă. Tranziţia stratului limită este însă simulată prea devreme de către ambele modele de turbulenţă, care au dificultăţi şi în simularea corectă a structurii undelor de şoc.*

The goal of this paper is to investigate the performances of the v2-f (*Lien and Durbin, 1996*) *and ζ-f* (*Hanjalic et al., 2004*) *turbulence models in predicting the external heat transfer distribution on a high turning turbine blade working in transonic regime at off design operating conditions. The turbulent heat flux was modeled first in the hypothesis of constant turbulent Prandtl number and secondly with the aid of the algebraic relation for turbulent thermal diffusivity of Rokni and Sunden* (*2003*)*. The numerical results show that the surface heat transfer coefficient is quite correctly predicted by both turbulence models in all the regions were the boundary layer is fully turbulent. Despite the realizable condition of Durbin, at the stagnation point the heat transfer rate remains over-predicted when the* Pr_t*=const. hypothesis is used, but the algebraic relation of Rokni and Sunden fixes this problem. Unfortunately, the boundary layer transition is simulated too early by both turbulence models, which also have some difficulties in predicting the real shock wave structure.*

Keywords: numerical simulation, external heat transfer, turbine blades

[1] Reader, Chair of Engineering Thermodynamics, University POLITEHNICA of Bucharest, Romania, e-mail: sdorin_ro@yahoo.com

[2] Prof., Chair of Engineering Thermodynamics, University POLITEHNICA of Bucharest, Romania

1. Introduction

Fluid flow and heat transfer fields through transonic passages of turbine blades cascades are extremely complicated. Favorable high pressure gradients due to the strong blade curvatures delay the boundary layer transition on the suction side and more often favor the re-laminarisation towards the end of blade pressure side. Beyond that, at off design operating regime, the inflow incidence angle is changed and the shock waves may appear. As a consequence, dramatic variations of convection heat transfer rate along the turbine blade exist.

To include the above effects in a numerical simulation, it is necessary to use the full Reynolds Averaged Navier-Stokes equations with appropriate models for turbulent momentum and turbulent heat fluxes. These models have to deal with boundary layer transition and shock wave-boundary layer interaction. Therefore, the Low Reynolds Number formulations of linear eddy viscosity models (LEVM), represent the minimal acceptable approach for this kind of flows.

The latest generation of LEVM uses in its formulation instead of damping functions the Kolmogorov time and length scales. Based on the elliptic relaxation concept, the $v2$-f turbulence model of Durbin [1] seems the most successful. It additionally includes another two equations, modeling the energy fluctuations $\overline{v^2}$ normal to the streamline, and a function f, related to the redistribution of turbulence energy from the stream-wise to the cross-stream flow direction. In order to gain in numerical stability, the original $v2$-f formulation was further modified by Lien and Durbin [2] without significant loss of accuracy. Then, with a little growth in the computational effort, the v^2-f model makes an important improvement in the numerical simulation of turbulent or transitional flows [3].

Using the same elliptic relaxation procedure, Hanjalic et al. [4] have derived the ζ-f turbulence model. Because of a simpler equation of the new variable $\zeta = \overline{v^2}/k$ and especially due to the wall boundary condition of f, the model becomes more robust and less sensitive to the non-uniformities of computational grid.

The goal of this paper is to explore the capability of $v2$-f and ζ-f turbulence models in predicting the flow and external convection heat transfer through a 2D passage of a high turning rotor blade working in transonic regime at off design operating conditions. The turbulent heat flux was first modelled in the hypothesis of a constant turbulent Prandtl number and secondly, with the aid of the algebraic relation for turbulent thermal diffusivity developed by Rokni and Sunden [5]. To validate our numerical simulation we have selected from the open literature, the experiments of Arts et al. [6], performed at a 2/1 scale on the RS1S blade of SNECMA.

2. Governing Equations

The mathematical model of steady state turbulent compressible flows consist of Reynolds averaged Navier-Stokes equations:

$$\frac{\partial \overline{\rho}\widetilde{u}_j}{\partial x_j} = 0 \tag{1}$$

$$\frac{\partial}{\partial x_j}\left[\overline{\rho}\widetilde{u}_i\widetilde{u}_j + p\delta_{ij} + \widetilde{\tau}_{ij} - \overline{\rho u_i'' u_j''}\right] = 0 \tag{2}$$

$$\frac{\partial}{\partial x_j}\left[\overline{\rho}\widetilde{u}_j\left(\widetilde{h}^* + k\right) + \widetilde{q}_j - \widetilde{u}_i\overline{\tau}_{ij} - \overline{\rho u_j'' h''}\right] = 0 \tag{3}$$

$$-\overline{\rho u_i'' u_j''} = \mu_t\widetilde{\tau}_{ij} - \frac{2}{3}\overline{\rho}k\delta_{ij} = 2\mu_t\left[\widetilde{S}_{ij} - \frac{1}{3}\delta_{ij}\frac{\partial u_k}{\partial x_k}\right] - \frac{2}{3}\overline{\rho}k\delta_{ij} \tag{4}$$

$$-\overline{\rho u_j'' h''} = \frac{\mu_t}{\mathrm{Pr}_t}\frac{\partial \widetilde{h}}{\partial x_j} \tag{5}$$

where $\widetilde{\varphi}$ is the Favre averaged part of φ.

The numerically friendly version of the original v^2-f model [2] is defined by the equations:

$$\mu_t = C_\mu \overline{\rho v^2}\tau_u \tag{6}$$

$$\frac{\partial}{\partial x_j}\left[\overline{\rho}\widetilde{u}_j k - (\mu + \mu_t)\frac{\partial k}{\partial x_j}\right] = \overline{\rho}P_k - \overline{\rho}\varepsilon \tag{7}$$

$$\frac{\partial}{\partial x_j}\left[\overline{\rho}\widetilde{u}_j\varepsilon - \left(\mu + \frac{\mu_t}{\sigma_\varepsilon}\right)\frac{\partial \varepsilon}{\partial x_j}\right] = \frac{\overline{\rho}}{\tau_u}\left(C_{\varepsilon 1}P_k - C_{\varepsilon 2}\varepsilon\right) \tag{8}$$

$$\frac{\partial}{\partial x_j}\left[\overline{\rho}\widetilde{u}_j\overline{v^2} - (\mu + \mu_t)\frac{\partial \overline{v^2}}{\partial x_j}\right] = \overline{\rho}\min\left\{kf^*, \varepsilon\left[\frac{2}{3}(C_1 - 1) + (6 - C_1)\frac{\overline{v^2}}{k}\right] + C_2 k\right\} - 6\overline{\rho}\frac{\overline{v^2}}{\tau_u} \tag{9}$$

$$-L^2\frac{\partial}{\partial x_j}\frac{\partial f^*}{\partial x_j} = \frac{1}{\tau_u}\left[\frac{2}{3}(C_1 - 1) + (6 - C_1)\frac{\overline{v^2}}{k}\right] + C_2\frac{P_k}{k} - f^* \tag{10}$$

In the above relations, τ_u and L represent the time and length scales of turbulence field computed as:

$$\tau_u = \min\left[\max\left(\frac{k}{\varepsilon}, 6\sqrt{\frac{\mu}{\rho\varepsilon}} \right), \frac{0.6k}{\sqrt{6}C_\mu \overline{v^2}\widetilde{S}^*} \right] \tag{11}$$

$$L = C_L \max\left[\min\left[\frac{k^{3/2}}{\varepsilon}, \frac{k^{3/2}}{\sqrt{6}C_\mu \overline{v^2}\widetilde{S}^*} \right], C_\eta \frac{\nu^{3/4}}{\varepsilon^{1/4}} \right] \tag{12}$$

It can be seen that both expressions contain the well known conditions of constraint for stagnating flows of Durbin [7]:

$$\tau_u \le \frac{0.6k}{\sqrt{6}C_\mu \overline{v^2}\widetilde{S}^*} \; ; \qquad L \le \frac{C_L k^{3/2}}{\sqrt{6}C_\mu \overline{v^2}\widetilde{S}^*} \tag{13}$$

applied to the time and length scales. Additionally it includes the realizability conditions for both, Davidson [8], ensuring that the generic normal stress $\overline{v^2}$ is always less than $2k/3$, and Sveningsson and Davidson [9], which use $6\overline{\rho}\overline{v^2}/\tau_u$ as a dissipation term of eq. (9) instead of the original $6\overline{\rho}\varepsilon_k/k$.

In the above relations, $\widetilde{S}^{*2} = \left(\widetilde{S}_{ij} - 1/3\,\delta_{ij}\partial u_k/\partial x_k\right)^2$, C_μ= 0.22, $C_{\varepsilon 2}$=1.9, C_1=1.4, C_2=0.3, C_L=0.23, C_η=0.85 are the model constants and:

$$C_{\varepsilon 1} = 1.4\left(1 + 0.045\sqrt{k/\overline{v^2}}\right) \tag{14}$$

The ζ-f model of Hanjalic et al. (2004) uses the variable $\zeta = \overline{v^2}/k$ instead of $\overline{v^2}$ and the equation of f is based on the Speziale formulation [10] of the quasi linear pressure strain model. The turbulent viscosity is computed as:

$$\mu_t = \overline{\rho} C_\mu \zeta k \tau_u \tag{15}$$

The k and ε equations remain the same as in the previous model, but the new equations of ζ and f are:

$$\frac{\partial}{\partial x_j}\left[\overline{\rho}\widetilde{u}_j\overline{\zeta}-\left(\mu+\frac{\mu_t}{\sigma_\zeta}\right)\frac{\partial\overline{\zeta}}{\partial x_j}\right]=\overline{\rho}f-\frac{\zeta}{k}\overline{\rho}P_k \tag{16}$$

$$-L^2\frac{\partial}{\partial x_j}\frac{\partial f}{\partial x_j}=-\frac{1}{\tau_u}\left(c_1+C_2'\frac{P_k}{\varepsilon}\right)\left(\zeta-\frac{2}{3}\right)-f \tag{17}$$

The constants of the model are C_μ= 0.22, $C_{\varepsilon 2}$=1.9, c_1=0.4, C'_2=0.65, C_L=0.36, C_η=0.85, and:

$$C_{\varepsilon 1}=1.4\left(1+0.012\sqrt{\zeta}\right) \tag{18}$$

This model allows for f the wall boundary condition f_w=-2$\nu\zeta/y^2$, which is more stable and robust from numerical point of view and, because of the modified f equation, improves the predictions of non-equilibrium wall flows.

As a reference for the numerical behaviour of the above two models, we choose the k-ω SST turbulence model of Menter [11].

The Reynolds averaged energy equation also needs to be closed. At a first time, this can be achieved with the aid of constant turbulent Prandtl number hypothesis, $Pr_t=\nu_t/\alpha_t$=0.85. As we will see later, the algebraic relation of Rokni and Sunden [5] for turbulent thermal diffusivity can be used.

3. Test cases definition

As pointed out above, we choose for numerical simulations the 2D turbine passage, experimentally tested by Arts et al. [6] at design and off design operating conditions. The original passage was build by mounting a high turning rotor blade (about 119 deg), having the chord c=35.906 mm, under a stager angle of 58.38 degrees and a pitch t/c=0.7607. The cascade model was manufactured at a scale 2/1 and was also used in the numerical simulations. For this work, two off design test cases were retained: 1) i=-5^o, M_{2is}=1.277, Re_{2is}=1.05x10^6; 2) i=+5^o, M_{2is}=1.124, Re_{2is}=1.06x10^6. Here, i denotes the incidence angle, $Re_{2is}=\rho_2 w_{2is} c/\mu_2$ and M_{2is} is the isentropic exit Mach number. In both cases we meet a transonic transitional flow and two shock waves appearing in the flow field. The main difference between the two experimental tests is the flow curvature, which is 10^o greater in the second case, determining an earlier boundary layer transition and stronger flow acceleration on the suction side of the blade.

4. Grid, boundary conditions and numerical procedures

A multi-block O-H type grid, with about 66000 nodes, was used for the calculation. This grid and some of its details around the leading and the trailing edges of the blades are shown in fig. 1. The O-type block of 604x58 (604 points around the blade) was used around the blade. In this inner block, the first 45 lines on the wall normal direction were built with an expansion factor of 1.07. The grid spacing at the blade was $1.5\text{x}10^{-4}$ cm, leading to a wall dimensionless coordinate $y^+=yu_\tau/\nu<0.7$ all around. Here, u_τ denotes the friction velocity, defined as $u_\tau^2 = \nu(\partial u/\partial y)_{y=0}$, where y is the normal distance to the wall. The number of point in the stream-wise direction is too high for a fully turbulent flow, but it was chose here in order to capture as well as possible the shock waves and boundary layer transition. It was obtained after three grid refinements, but the last one do not improved the numerical results.

Total temperature, T_{01}=417.5 K, total pressure, P_{01} and flow angle α were imposed at the inlet, and the static pressure p_2, with non reflecting boundary condition was set on the outlet. At the blade walls, no slip conditions were used for momentum, T_w=300K was set for energy equation, $k_w=0$, $\varepsilon_w=2\nu k/y^2$, $\overline{v_2}=0$, or $\zeta_w=0$ and $f_w^*=0$ or $f_w=-2\nu\zeta/y^2$ were imposed for the turbulent quantities appearing in the $v2$-f or ζ-f models.

The inlet value of the turbulent kinetic energy, k_∞ and that of the turbulent dissipation rate, ε_∞ were estimated from the relations [12]:

$$k_\infty = 1.5(Tu_\infty U_\infty)^2; \quad \varepsilon_\infty = C'_\mu k_\infty^{1.5} \big/ L_\infty \tag{19}$$

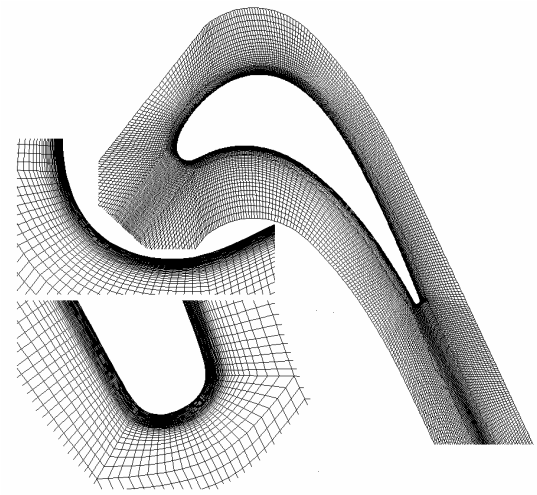

Fig. 1 Computational grid and some of its details around the leading and trailing edges of the blade

where Tu_∞ represents the turbulent intensity and L_∞=(0.001-0.01)t denotes the turbulence length scale. In all the test cases we set Tu_∞=4% and L_∞=0.01t, where t stands for the pitch. For these kinds of flows, a value of 4% for inlet turbulent intensity is large and determines the increment of heat transfer in both, the laminar and turbulent part of boundary layer and an earlier boundary layer transition. The $v2$-f and ζ-f turbulence models are also very sensitive to the inlet values of ε_∞. Therefore, the value of L_∞ was chosen after some numerical tests driven for M_{2is}=0.796, in which L_∞ was varied within the prescribed interval in order to obtain the best possible pressure side distribution of h [13]. For k-ω SST turbulence model, the value of ω_∞ was computed with the relation $\omega_\infty=\varepsilon_\infty/(C'_\mu k_\infty)$, where C'_μ=0.09.

The numerical computation was performed with the density based solver of the commercial code FLUENT 6.1.18 [14], in which both, v^2-f and ζ-f turbulence models were implemented through external subroutines. The implementation was verified in the case of turbulent flat plate boundary layers.

The density based scheme solves the continuity, momentum and energy equations in a coupled manner and uses the well known up-wind Roe procedure. For all the other equations, including those implemented through external subroutines, the solver uses a segregated numerical scheme. The second order spatial discretization scheme was used for every solved equation.

5. Numerical prediction of flow field.

Fig. 2 shows the Mach number contour of the flow. On the first half of the suction side, the flow is continuously accelerated until a certain supersonic velocity (about M=1.6) and the boundary layer remains in laminar state. As the acceleration slows down, the boundary layer undergoes a by-pass transition. Usually, vanes and rotor turbine blades are designed to operate free of shock waves. But at off design operating conditions they always appear. In our case, just

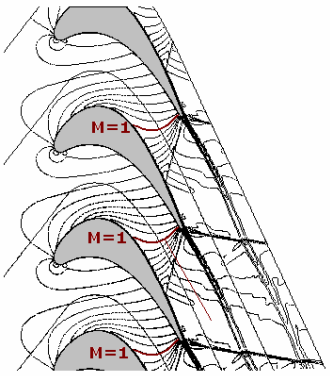

Fig. 2. Mach number contour, i=-5°, M_{2is}=1.277, Re_{2is}=1.05x10^6

behind the trailing edge of the blade, two shock waves come into view. Starting from the wake, the first one crosses the passage and intersects the suction side of the next blade. Because of the flow non-uniformity in cross-stream direction, its intensity decreases from the wake towards the suction side of the next blade, so that it is not reflected by the wall. The second wave, whose intensity is higher, is located outside the blade passage and intersects the wake generated by the forward blade. Behind the first wave, the velocity is nearly constant on the suction side and obvious the boundary layer remains turbulent.

On the first half of pressure side, the velocity growth is weak and the boundary layer is already turbulent. The flow is accelerated on the second half and reaches the sonic regime near the trailing edge of the blade.

6. Numerical prediction of convective heat transfer distributions

Analyzing the numerical results of the heat transfer coefficient, many issues should be discussed: 1) heat transfer in the impact point; 2) heat transfer distribution on the suction side, including the influence of the by-pass transition, shock wave-boundary layer interaction and of the turbulent flow behind the shock wave; 3) the heat transfer on the pressure side which occures in the turbulent regime.

Fig. 3 compares the experimental data and the numerical results of h for i=-5 deg, M_{2is}=1.277 and Re_{is}=1.05x10^6. The measured distributions reveal that the boundary layer transition on the suction side starts at s≈35mm and ends at s≈55mm. We can also observe the influence of the shock wave-boundary layer interaction on the heat transfer coefficient which appears at s≈88mm. As usual, on the pressure side, the boundary layer undergoes an early transition. Because of the negative incidence angle, a small recirculation bubble appears very close to the leading edge. It causes an important variation of h, but behind this region the

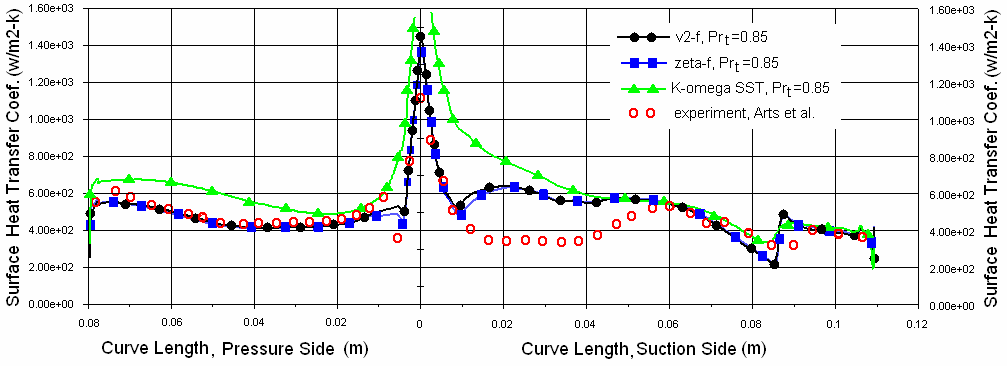

Fig. 3. Wall distribution of heat transfer coefficient, i=-5°, M_{2is}=1.277, Re_{2is}=1.05x10^6, $v2$-f and ζ-f turbulence models, Pr_t=0.85

developing boundary layer is clearly turbulent.

The Durbin's constraints (13) clearly improve the numerical prediction of h at leading edge stagnation point. While k-ω SST turbulence model furnishes a value of 67% greater than in reality, $v2$-f model decreases it only at 28%. More than that, a further improvement is obtained form the ζ-f model which reduces the error only at 20 %. Clearly the heat transfer coefficient at the leading edge still remains over-predicted, but the improvement brought by Durbin's restriction is evident.

The $v2$-f and ζ-f turbulence models also capture a part of laminar boundary layer developed on the suction side of the blade. Unfortunately, the transition is triggered earlier at $s\approx$9mm. As a consequence, at the locations where the boundary layer is laminar and is numerically predicted as turbulent, the simulated value of h is more than 1.6 greater than its measured values. All the turbulence models correctly simulate the suction side position of the shock wave, but they have some difficulties in describing the true flow structure resulting from the shock wave boundary layer interaction. As a consequence, a sharper and greater variation of heat transfer coefficient across the shock wave is predicted.

As opposed to k-ω model, which do not detect the small pressure side recirculation bubble, both $v2$-f and ζ-f models identify it. But despite the feasibility constraint of Durbin, the last two models still predict higher levels of turbulent kinetic energy in this area so that the distribution of h is clearly over-predicted. One of the possible causes of this behavior could be the position of the recirculation region just behind the location of the boundary layer transition, where the turbulence structure is not correctly described by the two models. Behind this region, the $v2$-f or ζ-f prediction of h fairly agrees with the experimental data in both, shape and absolute values. The exception occurs near the trailing edge, where the numerical values of the heat transfer coefficient appear lower than in reality. Clearly these models have some difficulties in predicting the wall fluxes under significant velocity accelerations, but obviously they perform a better this task than the k-ω SST model which, starting from the middle part of the pressure side, simulates a totally different shape of h.

Figure 4 shows the experimental and the computed distributions of h for i=+5 deg., M_{2is}=1.12 and Re_{2is}=1.06x10^6. In this test case, the flow turning angle was increased with about 10 degrees and the isentropic exit Mach number was slightly reduced. Here, only the $v2$-f and ζ-f turbulence models were retained for the numerical simulations. By comparison with the previous case, the agreement of computed heat transfer coefficient with the experimental data is better on the suction side and lower, but acceptable, on the pressure side. Obviously, the prediction problems of h in the stagnation point and across the shock wave still remains, and beyond that the position of the shock wave is simulated a little downstream than its real location. On the other hand, figs. 3 and 4 show that the

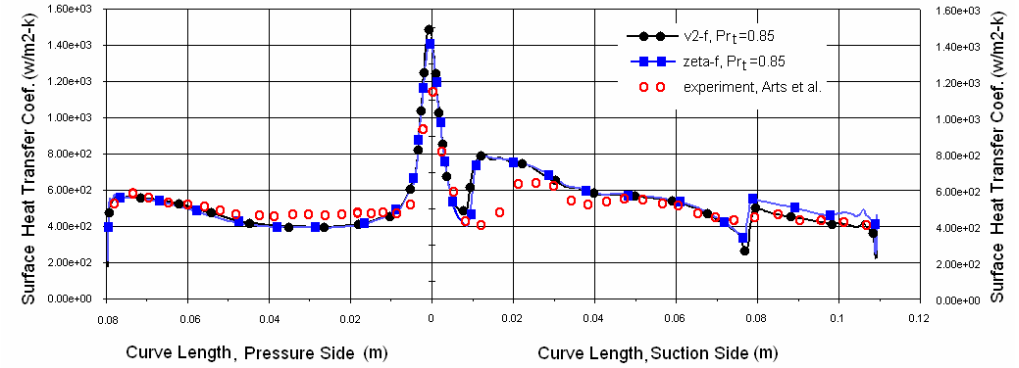

Fig. 4. Wall distribution of heat transfer coefficient, i=+5°, M_{2is}=1.124, Re_{2is}=1.06x10^6, $v2$-f and ζ-f turbulence models, Pr_t=0.85

predicted starting point of transition, which in both cases is numerically simulated at about 9mm from the leading edge stagnation point, is quite insensitive to the incidence angle. The differences between the two test cases appear only during boundary layer transition and behind it.

7. Improving the heat transfer prediction in the stagnation point

The assumption of constant turbulent Prandtl number relies on the analogy between velocity and thermal boundary layers. But this assumption does not hold in the vicinity of the flow stagnation point.

In the absence of a two equations eddy diffusivity model for turbulent heat flux especially designed for $v2$-f of ζ-f models we choose to compute the turbulent thermal diffusivity with the algebraic relation of Rokni and Sunden [5]:

$$\alpha_t = C_\lambda \left[1-\exp\left(-\mathrm{Re}_\varepsilon/14\right)\right]\left[1-\exp\left(-\sqrt{\mathrm{Pr}}\,\mathrm{Re}_\varepsilon/14\right)\right]\cdot \\ \cdot\left\{0.83\left(k^2/\varepsilon_k\right)+2.51k^{0.5}\left(\nu^3/\varepsilon_k\right)^{0.25}\mathrm{Pr}^{-1}\exp\left[-\left(\mathrm{Re}_t/200\right)^2\right]\right\} \tag{20}$$

where $\mathrm{Re}_\varepsilon=u_\varepsilon y/\nu$, $\mathrm{Re}_t=k^2/\nu\varepsilon_k$, and $u_\varepsilon=(\nu\varepsilon_k)^{0.25}$. Note that this relation was derived from the well known model of Abe [15], by considering a constant value for the turbulent time scale ratio $R=\tau_t/\tau_u$=0.7, where τ_θ is the time scale of fluctuating temperature field.

Figure 5 presents the simulated distributions of h by the $v2$-f turbulence model and the algebraic relation of Rokni and Sunden. In the stagnation point, the agreement with the experimental data is very good. Some improvements can be

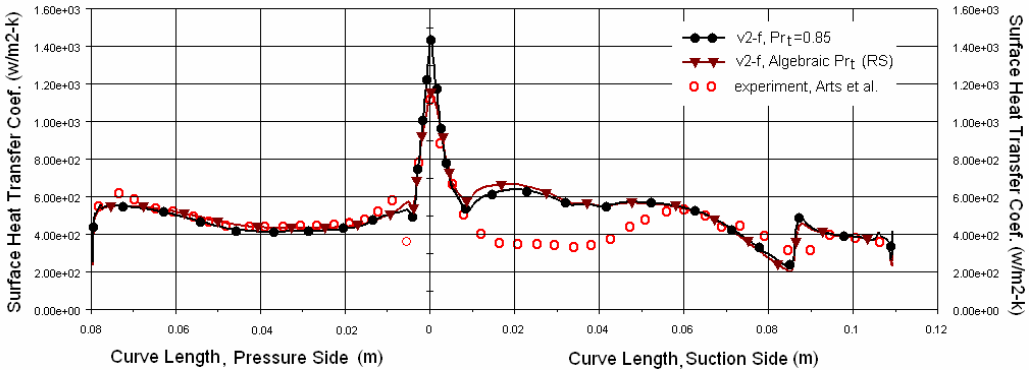

Fig. 5. Computed wall distribution of h, using Prt=const. hypothesis or Rokni&Sunden algebraic relation, $v2$-f turbulence model, i=-5°, M_{2is}=1.277, Re_{2is}=1.05x10^6

observed along the pressure side because there the boundary layer is fully turbulent. Obviously on the suction side, the problem of transition still remains, but in the simulated laminar or turbulent parts of boundary layer, the relation (19) works well. .

8. Conclusion

In this paper, we have investigated the capability of $v2$-f and ζ-f eddy viscosity models to numerically describe the external heat transfer on transonic turbine blades working at off design operating conditions. The numerical results showed that both turbulence models prescribe quite correctly the heat transfer coefficient on the blade surfaces where boundary layer is fully turbulent. They also capture a part of laminar boundary layer developed on the suction side of the blade, but the transition is triggered to early. The position of internal shock wave is properly predicted, but the real structure of wave-boundary layer interaction is not well seized. The constraint condition of Durbin (13) clearly improves the prediction of the heat transfer coefficient in the stagnation point, but its value remains over-estimated when the turbulent heat flux is modeled with the classical hypothesis of constant turbulent Prandtl number. Some little improvements of calculation are obtained from ζ-f model at the stagnation point and in the boundary layer transition. Also the elliptic relaxation eddy viscosity models deal better with the heat transfer prediction on the transonic turbine blades than the classical k-ω models.

The algebraic relation for turbulent thermal diffusivity of Rokni and Sunden completely fix the problem of heat transfer prediction in the stagnation

point of the flow and brings some improvement of heat transfer distribution on the pressure side of the blade.

B I B L I O G R A P H Y

[1] *P. A. Durbin,* Separated flow computation with the k-ε-v^2 model, AIAA J. **33** (1995) 659-664

[2] *F. S. Lien, P. A. Durbin*: Non-linear k-ε-v^2 modeling with application to high lift, Annual Research Brifs, Center for Turbulence Research, (1996), eg. pp. 5-22.

[3] *F. S. Lien, G. Kalitzin, P. A. Durbin,* RANS modeling for compressible and transitional flows, Annual Research Brifs, Center for Turbulence Research, (1998), eg. pp. 267-286

[4] *K. Hanjalic, M. Popovac, M. Hadziabdic,* A Robust Near Wall Eliptic-Relaxation Eddy-Viscosity Turbulence Model for CFD, International Journal of Heat and Fluid Flow, **25**(2004), 1047-1051.

[5] *M. Rokni, B. Sunden,* Investigation of a Two-Equation Turbulent Heat Transfer Model Applied to Ducts, J. Heat Transfer **125** (2003) 194-200

[6] *T. Arts, J.M. Duboue, G. Rollin,* Aero-thermal performance measurements and analysis of a two dimensional high turning rotor blade, Turbo Expo Conference, Orlando Florida USA, (1997), ASME Paper No. 97-GT-120.

[7] *P. A. Durbin*: On the k-ε stagnation point anomaly, Int. J. Heat and Fluid Flow, 17 (1996) 89-90.

[8] *L. Davidson, P. Nielsen, A. Sveningsson*: Modification of v^2-f model for computing the flow in a 3D wall jet, in Turbulence Heat and Mass Transfer 4 (Hanjalic et al. eds.) New York Walling Ford (2003), 577-584.

[9] *A. Sveningsson, L. Davidson,* Assessement of realizability constraint in v^2-f turbulence models, Int. J. Heat and Fluid Flow, **25** (2004), 785-794

[10] *C. G. Speziale, S. Sarkar, T. Gatski,* Modelling the pressure-strain correlation of turbulence: an invariant system dynamic approach, J. Fluid mech., 227 (1991), 245-272.

[11] *F. R. Menter*: Two Equation Eddy-Viscosity Turbulence Models for Engineering Applications, AIAA J., **52** (1994), 1598-1606

[12] *R. F. Kunz, B. Lakshminarayana,* Three-Dimensional Navier-Stokes Computation of Turbomachinery Flows Using an Explicit Numerical Procedure and a Coupled k-ε Turbulence Model, Journal of Turbomachinery, **114** (1992), 627-642.

[13] *D. Stanciu, M, Marinescu,* Reynolds Averaged Navier-Stokes based numerical simulation of external heat convection and losses for transitional subsonic flows through a 2D turbine passage, Int. J. Energy Technology and Policy, 6(2008), nos ½, 31-46.

[14] *Fluent Inc*.: User,s Guide, Fluent Incorporated, 1998

[15] *K. Abe, T. Kondoh, Y. Nagano,* A New Turbulence Model for Predicting Fluid Flow anf Heat Transfer in Separating and Reattaching flows-II. Thermal Field Calculation, Int. J. Heat Mass Transfer, vol 38 (1995), no. 8, 1467-1481.